AD

TECHNICAL REPORT ARCCB-TR-99016

GRAY LAYERS AND THE EROSION OF CHROMIUM PLATED GUN BORE SURFACES

PAUL J. COTE
CHRISTOPHER RICKARD

SEPTEMBER 1999

US ARMY ARMAMENT RESEARCH,
DEVELOPMENT AND ENGINEERING CENTER
CLOSE COMBAT ARMAMENTS CENTER
BENÉT LABORATORIES
WATERVLIET, N.Y. 12189-4050

DISCLAIMER

The findings in this report are not to be construed as an official Department of the Army position unless so designated by other authorized documents.

The use of trade name(s) and/or manufacturer(s) does not constitute an official endorsement or approval.

DESTRUCTION NOTICE

For classified documents, follow the procedures in DoD 5200.22-M, Industrial Security Manual, Section II-19, or DoD 5200.1-R, Information Security Program Regulation, Chapter IX.

For unclassified, limited documents, destroy by any method that will prevent disclosure of contents or reconstruction of the document.

For unclassified, unlimited documents, destroy when the report is no longer needed. Do not return it to the originator.

REPORT DOCUMENTATION PAGE

Form Approved
OMB No. 0704-0188

1. AGENCY USE ONLY *(Leave blank)*	2. REPORT DATE	3. REPORT TYPE AND DATES COVERED
	September 1999	Final

4. TITLE AND SUBTITLE

GRAY LAYERS AND THE EROSION OF CHROMIUM PLATED GUN BORE SURFACES

5. FUNDING NUMBERS

AMCMS No. 6226.24.H191.1

6. AUTHOR(S)

Paul J. Cote and Christopher Rickard

7. PERFORMING ORGANIZATION NAME(S) AND ADDRESS(ES)

U.S. Army ARDEC
Benet Laboratories, AMSTA-AR-CCB-O
Watervliet, NY 12189-4050

8. PERFORMING ORGANIZATION REPORT NUMBER

ARCCB-TR-99016

9. SPONSORING / MONITORING AGENCY NAME(S) AND ADDRESS(ES)

U.S. Army ARDEC
Close Combat Armaments Center
Picatinny Arsenal, NJ 07806-5000

10. SPONSORING / MONITORING AGENCY REPORT NUMBER

11. SUPPLEMENTARY NOTES

12a. DISTRIBUTION / AVAILABILITY STATEMENT

Approved for public release; distribution unlimited.

12b. DISTRIBUTION CODE

13. ABSTRACT *(Maximum 200 words)*

The present report describes observations and analyses in a survey study of erosion damage in chromium plated gun bore surfaces. Sections of three fired chromium plated 120-mm M256 gun tubes and two 155-mm gun tubes (M199 and XM297) were examined by optical microscopy, laser scanning confocal microscopy (LSCM), and electron microprobe analyses. These tubes experienced significant erosion damage and chromium loss. A rifled portion of the 155-mm M199 tube was plated with low contractile (LC) chromium and the 155-mm XM297 and 120-mm M256 tubes were plated with high contractile (HC) chromium.

New insights regarding the erosion process and the origin of chromium loss are obtained by investigation of the initial damage to the steel at the tips of the fine cracks in the chromium. Reaction products from gas-metal interactions at the gun bore surface are normally difficult to find because of gas wash effects. Examination of unetched specimens from a variety of fired tubes shows that these products remain in place in the relatively protected regions beneath the chromium when chromium crack widths are small. The initial damage is manifested as gray layers or gray regions in the steel at the tips of the fine chromium cracks. Electron microprobe analyses indicate that these gray layers are composed of iron sulfide, iron oxide, or mixtures of the two compounds.

14. SUBJECT TERMS

Erosion, High Contractile Chromium, Low Contractile Chromium, Iron Sulfide, Iron Oxide, Chromium Spallation, White Layers

15. NUMBER OF PAGES

18

16. PRICE CODE

17. SECURITY CLASSIFICATION OF REPORT	18. SECURITY CLASSIFICATION OF THIS PAGE	19. SECURITY CLASSIFICATION OF ABSTRACT	20. LIMITATION OF ABSTRACT
UNCLASSIFIED	UNCLASSIFIED	UNCLASSIFIED	UL

TABLE OF CONTENTS

ACKNOWLEDGEMENTS

The authors thank Greg Vigilante and Gay Kendall for their assistance in various phases of this work. Thanks are due to Sam Sopok and George Pflegl for consultative assistance and for supplying several of the specimens.

INTRODUCTION

The 1946 National Defense Research Committee report, "Hypervelocity Guns and the Control of Gun Erosion," (ref 1) is a major compilation of work that elucidates the main features of the erosion process in gun bores. More recent reviews include "The Problem of Gun Bore Erosion: An Overview" by Ahmad (ref 2), and the Proceedings of the 1996 Sagamore Workshop on Gun Barrel Wear and Erosion (ref 3).

There is a consensus that the dominant factor controlling erosion rate is the flame temperature of the propellant gas. Melting is considered the most rapid erosion mechanism and is expected at the highest propellant temperatures. One also expects melting in regions of high turbulence, such as chromium pits, where heat transfer from the hot gas core is high.

Gas-metal reactions (Table 1) are next on the list of major factors, with high-temperature chemical attack expected from several of the propellant gas constituents. The ubiquitous white layers on bore surfaces suggest that carbon attack is a significant chemical factor in gun bore erosion. The formation, melting, and removal of low melting temperature carbide is the assumed primary erosive mechanism of carbon attack.

Table 1. Erosion-Related Chemical Reactions

Major Propellant Gas Products	CO, CO_2, H_2, H_2O, N_2, H_2S from Additives (e.g., K_2SO_4)
Water-Gas Reaction	$CO_2 + H_2 = CO + H_2O$
Carbon Deposition	$2CO = C + CO_2$
Iron Oxide Formation	$Fe + CO_2 = FeO + CO$
Carbide Formation	$3Fe + 2CO = Fe_3C + CO_2$
Iron Sulfide Formation	$Fe + H_2S = FeS + H_2$

Another observed high-temperature chemical reaction is steel oxidation. Spalling of the weak, brittle, iron oxide scale is the assumed mechanism of material removal in this case.

Iron sulfide formation is yet another high-temperature reaction that can damage the bore surface. Vented combustor simulation tests previously indicated that sulfur, even in small quantities, caused such severe erosive effects that removal of all sulfur sources was recommended (ref 1). As an illustration of the difficulties in understanding erosion phenomena, other laboratory simulations (ref 4) have suggested that sulfur additions cause relatively modest effects in contrast to earlier reports (ref 1). Sulfur additions have actually been beneficial at higher vented combustor pressures.

It has also been suggested (ref 5) that hydrogen embrittlement may cause cracking and initiate substrate erosion. Hydrogen cracking, which occurs near room temperature, may develop after firing because of residual tensile stresses generated in the first few mils of the steel from the familiar "thermal shock" effect.

Although chemical equilibrium may not occur in the millisecond time frame of erosion processes, equilibrium is often assumed in order to indicate how reactions might occur (ref 1). For example, under equilibrium conditions for the water-gas reaction in the chamber (Table 1), oxidation of steel is expected at high temperatures when the carbon dioxide-carbon monoxide ratios are high; at lower temperatures, low ratios are predicted and carbon deposition and carburization are expected. The omnipresent white layers indicate that a carburizing atmosphere is generally maintained during firing.

Despite extensive studies, the extreme environment within the gun tube during firing, the variety of gaseous constituents, and the complexity and nonequilibrium nature of the gas-metal reactions during firing all serve to obscure many features of the erosion process. Consequently, the erosion process is likely to be unpredictable in any given case. Basic issues have yet to be resolved. Thus, the field of gun bore erosion remains largely an empirical science: testing of actual rounds in actual tubes is still necessary.

At present, the only viable means of protection against erosion on gun bore surfaces is the use of additives, such as talc or titanium dioxide, along with chromium electrodeposition of the bore surface. Intermediate electrodeposited layers (nickel, copper, and cobalt) were tested in the past (ref 1) as undercoatings for the microcracked chromium. Only cobalt showed sufficient chemical resistance to be effective.

Erosion of chromium plated tubes is initiated by chromium removal (evidently by spallation), which allows hot gas attack of the unprotected substrate steel. During the electrodeposition process and subsequent heat treatment to outgas hydrogen, the chromium deposit develops a network of microcracks. Prior to firing, chromium microcracks do not extend through the chromium thickness, but, instead, terminate within the chromium.

For high contractile (HC) chromium, most chromium cracks originate and terminate within the chromium plate (embedded cracks) as a result of continuous crack formation and crack healing by rapid deposition at the crack edges during the deposition process (ref 6). With exposure to high temperatures during firing, the microcracks grow, and the surface microcracks, in particular, propagate through the chromium to the steel substrate, so that the original chromium deposit becomes, in effect, an assembly of individual, isolated islands. Inspection of fired gun bore surfaces in the present study indicates that the spalling process proceeds from this configuration by progressive removal of the individual isolated chromium islands through metal failure at or near the chromium/steel interface.

The focus of the present study is on the initiation of damage to the steel beneath the chromium. It is found that, at the initial stages of erosion damage to the steel, the reaction products remain in place in a relatively protected environment at the chromium crack tips; this permits direct observation of one of the key mechanisms of chromium spallation.

EXPERIMENTAL PROCEDURE

High magnification examination of metallographically-prepared unetched specimens from different chromium plated bore surfaces from fired tubes showed similar gray regions immediately beneath the chromium at the tips of chromium microcracks. These products can be dissolved and partially removed by the etching process to give the appearance of wide cracks or erosion pits. With unetched specimens, these gray regions may be mistaken for cracks filled with firing debris or attributed to white layers (ref 7), but closer study shows that they are gas-steel reaction products maintained in their location by the relatively-protected environment beneath the chromium. Following is a brief summary of results of an examination of these reaction products for five representative tubes.

Specimens were cut and prepared in the usual manner from the fired tubes to permit study of the progress of erosion through the chromium and into the steel. Since the focus is on initiation of damage in the steel, high magnification (500 to 3000X) was generally used to observe and record the effects. For several fired specimens, the chromium plate was electrolytically removed using KCl + KOH aqueous solution to permit examination of the erosion process into the chromium/steel interface plane through the network of chromium microcracks.

Specimen 1 was obtained from a 120-mm tube with 1246 fired conventional rounds; the specimen was cut from an axial position at 22 inches from the rear face of the tube (RFT). Specimen 2 was obtained from a 120-mm tube with approximately 80 experimental high-temperature rounds and 220 conventional rounds; specimen location was 22 inches from RFT. Specimen 3 was obtained from a 120-mm tube with 424 conventional rounds; specimen location was 17 inches from RFT. (This tube was used for lot acceptance testing and taken out of service when shot dispersion became excessive.) Specimen 4 was obtained from the M199 155-mm howitzer where the rifled surface had been plated with low contractile (LC) chromium. Approximately 3000 conventional rounds were fired through this tube; specimen location was 38 inches from RFT. Specimen 5 was obtained from the HC chromium plated 155-mm XM297 with 495 conventional rounds fired in a "rapid fire" mode; specimen location was 103 inches from RFT.

Laser scanning confocal microscopy (LSCM) was used to perform a general survey of the dimensions of the spalled patches in the chromium to assess the depth and width of the spalled islands of chromium and the dimensions of the pits beneath the chromium. The LSCM was also used for general microscopy and imaging.

Electron microprobe energy dispersive spectroscopy (EDS) was used to establish the chemical composition of the reaction products in the chromium cracks and at the tips of the chromium cracks in the steel. Electron microprobe wavelength dispersive spectroscopy was used to supplement EDS measurements. These techniques do not identify specific compounds so in our study, identification of constituents as compounds is based on the relative intensities of the x-ray emissions and homogeneity of the chemical distributions in the gray layers.

RESULTS

Figure 1 is a photomicrograph showing erosion damage of specimen 1 at the chromium/steel interface after about 1200 conventional rounds. The dark areas at the tips of the chromium cracks are gas-steel reaction products. An unetched specimen was examined to more clearly delineate the reaction product, which appears as a solid gray material under optical microscopy. Metal attack clearly occurs via gas ingress through the fine cracks in the chromium plate. Energy dispersive spectroscopy indicates that the gray material is a mix of iron oxide and iron sulfide.

Figure 2 is an unetched micrograph from specimen 2 after approximately 80 high-temperature experimental rounds. The figure shows that the gas-steel reaction product can, in some instances, extend for large distances along the interface.

Figure 3 is a micrograph of an etched section from specimen 2. There is substantial removal of the gray material from the etching process (demonstrating that this is not a white layer), so that the pitting becomes more clearly defined. A heat-affected zone is seen in this micrograph. It can also be seen that a true white layer exists at the interface between the gray material and the steel. The white layer is only observable within heat-affected zones after etching. The gray material is partially removed by the etching process known as a Nital etch. The gray material is also removed by exposure to a drop of concentrated phosphoric acid, which leaves the surrounding steel and white layer unaffected. This ready attack by weak acid solutions is further evidence of a steel reaction product.

Another observation reflected in Figures 1 through 3 is that the decomposition pits can join up along the steel/chromium interface as the pits grow into the steel. Such chemical attack is obviously a major disbonding mechanism for chromium spallation.

Figure 4 is a micrograph of a severely eroded area from specimen 2. There is a total chromium loss at this area, and the erosion process removed approximately a 5-mm layer of the steel at this location. A thin white layer can be seen at the steel surface, and extensive white layer formation occurs around the deep pits in the steel. This is known to represent fine-grained retained austenite stabilized by carbon and nitrogen with precipitates (primarily carbides) distributed throughout the retained austenite. The reaction products that form in the protected regions beneath the chromium a few millimeters away, as shown in Figure 3, are absent in this highly eroded area.

Figure 5 is a micrograph of an etched section from specimen 2 that was used for EDS chemical analysis. The chemical composition shows that the indicated compounds occur as part of the gray decomposition products. The white layer forms as a thin bright layer at the steel surface. It is known to be an austenite layer in the steel with carbide precipitates. Immediately adjacent to this white layer is an iron sulfide layer, which runs all along the pit surface and extends to the blunt tip of the pit, well beyond the heat-affected zone. The depth of the corrosion pit in the steel is approximately 100 microns. The reaction product covers the entire surface and thus forms at high temperatures during firing. At the core of the pit is a zone of iron oxide with

no evidence of sulfide. A mixture of talc and other debris is also seen in the core region in this case. Similar features are seen in all the other erosion pits on this specimen. Occasionally iron oxides and iron sulfides appear to be mixed together. The small pocket reaction zone at the tip of the fine chromium crack in Figure 5 shows the earliest stages of chemical attack. Only iron oxide is observed in this case. The initial progress of chemical attack radially into the gun tube appears to occur through fissures in the thick oxide or sulfide layers.

Figure 6 is a micrograph of an unetched section from specimen 3 (120-mm, 424 conventional rounds—approximately an equal mix of M829 and M829A2 rounds). Again the features are the same with gray reaction zones at the tips of the chromium microcracks. Energy dispersive spectroscopy shows the gray zones contain only iron oxide.

Figure 7 consists of micrographs of an unetched section from specimen 4 at 2000X and 400X. This section is from the LC plated 155-mm specimen. The numerous fine embedded cracks that occur between the major cracks with HC chromium are absent. In this case, the gray layers often exhibit a distinct yellow tint. Energy dispersive spectroscopy shows only iron and sulfur, indicating that the gray/yellow reaction zones are sulfides. The sulfur likely originates from the potassium and/or sodium sulfate used as a flame suppressant in the 155-mm.

Another significant observation is that the surface cracks are all nearly completely filled with a dark glossy material in which particles appear to be embedded. Energy dispersive spectroscopy shows this material to be primarily magnesium, silicon, and oxygen, which are the constituents of the talc additive added to the combustible case of the 120-mm. The same material forms on the top surface of the chromium, but is lighter in color and quite transparent. The glossy solid nature of this coating indicates deposition as molten talc. Subsequent rapid solidification of the talc can be seen to form a protective glaze along the chromium surface and in the chromium cracks and steel pits beneath the chromium. This thin glaze can be dissolved with a drop of concentrated phosphoric acid on a heated specimen (~50°C) in approximately 30 minutes (ref 8), which is useful for revealing the surface crack patterns.

A similar dark glossy coating forms on the 155-mm chromium and extends into the chromium cracks and steel corrosion pits. Energy dispersive spectroscopy shows this to be primarily titanium oxide, which also appears to be deposited everywhere initially as a molten layer extending deep into the steel pits.

Figure 8 is a micrograph of the bore surface from specimen 2 where all of the chromium coating has been electrochemically stripped away from the steel substrate. It is seen that the entire array of large and small cracks that are present in the chromium are replicated in the erosion pattern in the steel. From this specimen orientation, all of the major fracture-like features in the steel are also solidly filled with the same dark glaze-like material (along with many of the fine crack-like features). This supports the observations regarding crack filling described above. From the previous analysis of the same tube, the dark fill material is known to be predominantly talc.

The original chromium layer in Figure 8 was heavily spalled prior to stripping this specimen. The nature of the spalling is a removal of numerous individual islands of chromium whose boundary is determined by the major chromium cracks. In the initial stages of spallation, the chromium has the appearance of being heavily pitted with many small pits visible without magnification. After stripping away the chromium, there is no evidence of pitting or spallation extending into the steel substrate; thus, the spallation of the chromium does not originate by fracture of the steel. This is in accordance with LCSM inspection of dozens of spalled regions, which show the depth of the spalls extending no deeper than the chromium/steel interface zone. Usually, in both the LC and HC specimens, fragments of chromium are observed adhering to the steel at the flat bottom of the spalled regions showing that the spallation originated from metal failure in the chromium or at the chromium/steel interface region.

Figure 8 also shows that the erosion of the steel occurs as closed paths around rounded chromium islands. These paths extend into the steel as chemical attack drives the "heat-checking" process through the chromium cracks and into the steel. It has been observed that the depth of penetration of damage can be orientation-dependent (ref 5).

In specimen 4 (LC chromium on the 155-mm M199), the spallation fragments are significantly larger than those of all the HC specimens, thus reflecting a lower initial crack density. The top surfaces of the chromium plate on the lands are severely scratched and worn, indicating that sliding wear is the chromium spallation mechanism in the LC 155-mm specimen. Further evidence of a wear mechanism is that there is no spallation in the grooves. As shown in Figure 7, with LC chromium, one does not observe the widespread undermining of the chromium through a high density of microcracks as seen with HC chromium.

In specimen 5 (HC chromium plated 155-mm XM297), the cross section (not shown) reveals the same general features as observed with the 120-mm HC chromium plated specimens. These specimens feature similar gray reaction zones at the initiation of damage, along with many of the larger crack-like features. There is also evidence of gas penetration into the steel through the network of fine cracks between the major cracks, which is similar to what occurs with the HC chromium plated 120-mm. Microprobe analysis indicates that the gray material is composed of a mix of iron sulfide and iron oxide.

Another significant difference between the 155-mm LC and HC chromium crack patterns and those observed on the HC chromium plated 120-mm and other 155-mm plated tubes is the predominance of cracks oriented perpendicular to the wear direction. The HC chromium crack pattern of specimen 5 (155-mm XM297) consists of large cracks perpendicular to the wear direction, but these are superimposed upon the standard HC chromium microcracks that are present initially in all HC chromium plated tubes. The standard HC chromium plated surfaces all resemble the chromium crack pattern indicated in Figure 8 where the chromium islands are seen to have more random, rounded shapes. By contrast, on the LC chromium plated 155-mm tube, rectangular shapes predominate that are clearly aligned with the wear direction. The HC chromium plated 155-mm XM297 at the 103-inch position has a system of large cracks aligned perpendicular to the wear direction, where the large crack widths appear to originate from chromium spallation because the steel beneath the large cracks appears to be mainly intact.

SUMMARY OF OBSERVATIONS

Transverse sections of laboratory specimens and fired specimens of HC chromium show a high density of embedded microcracks between the major cracks in the chromium. These embedded microcracks are absent in fired LC chromium specimens.

The enlargement of chromium cracks during firing permits access of hot propellant gas to the steel. As a consequence, the chromium coating serves as an etching mask, allowing chemical attack of the steel through all the major and minor microcracks in the chromium.

The damage to the steel generally initiates through chromium cracks by chemical attack, as evidenced by the presence of gray layers (sulfides, oxides) at the chromium crack tips. In heat-affected zones, one also observes the white layer in the steel adjacent to the oxide or sulfide gray layer. Fine cracks in the steel substrate are rare, especially in the first five or ten mils. Examination at higher magnifications shows that the features that appear to be fractures under low magnification are actually regions where substantial volumes of steel were consumed by chemical attack. These features often terminate as blunt pits coated with oxide or sulfide compounds. Fissures are generally observed in the thick brittle gray layers.

Except where the gray sulfide or oxide reaction products completely fill the reaction zone, the microcracks in the chromium and the extensions of these cracks into the steel are generally completely filled with the protective additives and other debris. This filling often extends up to the blunt tips of the fracture-like features.

When the chromium crack widths are large, the pits in the steel are correspondingly large and gray layers are sometimes not observed. In these cases, reaction products are presumably incorporated into or obscured by the fill material. In other cases, substantial zones of the gray products can be found in the steel all along the boundary of even the largest pits in the specimen.

DISCUSSION

An attempt was made in our study to examine and accurately represent general features and trends for damage initiation in the steel substrate beneath the chromium plate. Features that occur infrequently or are clearly anomalous are omitted from discussion. These include instances, for example, where rotating band material or sabot material penetrates chromium cracks. Also, no data are presented for damage extending beyond five mils into the steel. The data are from specimens cut from a breech end location where substantial erosion occurred so that other failure modes may be present at other positions along the given tube; any generalizations should be viewed in this context.

The main reaction product observed on unplated gun bore surfaces is the white layer with its well-documented features (ref 10). The new data regarding the gray layers (oxides and sulfides) in eroded zones beneath the chromium plate are relevant to the chromium spallation mechanism. Results show that this phenomenon occurs in both tank guns and howitzers. (Sopok [ref 11] had earlier observed mixtures of oxides, sulfides, and carbides in bore surface residues and in crack wall layers of the M242 Bushmaster.) The focus of this study is initiation of damage to the steel beneath chromium, since the key function of bore protective coatings is minimization of damage initiation. Another reason for the focus on initiation is that at the later stages of propagation of damage into the steel, the pitted zones become filled with additive material and other debris and so that the gas-steel reaction products can be obscured.

The propagation of damage through the chromium and into the steel is clearly by chemical attack of the steel beneath the chromium. Figure 8 illustrates that the damage to the steel substrate is a high-temperature etching process so that the chromium plate serves, in effect, as an etching mask. Chemical attack forms relatively large, often isotropic volumes of reaction product at the chromium crack tip. The terms "pocket erosion" and "mushrooming" have been coined for the advanced stages of this phenomenon (ref 1) in gun tubes. A similar phenomenon, termed "ballooning oxidation," occurs with hot corrosion beneath coating cracks in gas turbines (ref 12). There are also indications that the gray layers can propagate along grain boundaries by occasional observations of fine lines of gray reaction products extending from the main erosion pits.

Stress and fracture of uncorroded steel are not central factors in the initiation of damage into steel at the chromium/steel interface. Fracture appears to play a secondary role by the development of fissures through reaction products. Fine cracks in the steel are rare in the first several mils. Most of the fracture-like features in the first 5 or 10 mils beneath the chromium are more accurately viewed as resulting from combined bulk and grain boundary chemical attack and thus form extended corrosion zones. This type of bulk and grain boundary chemical attack involving formation of sulfide and oxide layers is also seen in hot corrosion in gas turbines (ref 12), for example.

Similarly, the present observations of the initiation and gradual progression of oxygen and sulfur attack into the steel do not support the suggestion that hydrogen cracking of the steel, after firing, initiates failure of the chromium (ref 5). The driving force for the proposed room temperature hydrogen cracking mechanism is a layer of tensile residual stress in the steel, generated by the "thermal shock" process. Since this stress layer is present after the first round, the distinguishing feature of the proposed hydrogen-cracking mechanism is fine cracks extending several mils into the steel through the highest stressed layers after the first few rounds. Experimental evidence in support of this predicted hydrogen-assisted cracking mechanism has been found (ref 13) in laboratory simulations by laser pulse heating (single pulse) of hydrogen-embrittled steel (by the chromium deposition process). On the other hand, as discussed earlier, no evidence is found for cracking as the initiation of damage into the steel in actual gun bore surfaces. Furthermore, as the chromium stripping experiment (Figure 8) shows, spallation does not occur by joining of cracks in the steel.

As the corrosion pits deepen, a transition is expected where chemical effects become insignificant and mechanical fatigue and fracture processes begin. This is a basic assumption in the full-scale simulation testing used to establish safe service lives of gun tubes, where field firing is used to obtain initial heat-checking damage. The location of this transition must vary with gas flame temperature, pressure, and propellant composition.

Regarding the specifics of chemical attack, carburization, as indicated by white layers, appears to be ubiquitous. The fact that only the white layer is detected along the exposed outer bare steel areas (Figure 4) is in contrast to the reaction areas a few millimeters away under the chromium where carbon, oxygen, and sulfur layers form. This illustrates the difficulty in analyzing gun bore erosion. Surface reaction products are normally swept away in the process.

The reaction product that forms adjacent to the white layer is likely to depend on the nature and quantity of the sulfur additives used (e.g., flame suppressant, black powder igniter). All sulfur additives are converted to hydrogen sulfide in the propellant gas, and gun bore surfaces may be severely attacked with even small quantities of hydrogen sulfide (ref 1). It is also known that small amounts of hydrogen sulfide can severely attack grain boundaries at high temperatures (ref 12). The present data demonstrate that hydrogen sulfide is very reactive and damaging beneath the chromium, since the amount of sulfur in the additives is generally less than one percent (ref 3) of the total propellant weight.

As the chromium cracks widen and the corrosion pits in the underlying steel enlarge, the chromium cracks and steel pits become filled, mainly with protective additives (apparently deposited in the molten state along with other debris). The presence of protective additives in the corrosion pits should be beneficial, since it reduces the volume of hot propellant gases delivered to the corrosion pits. The effectiveness of the additive in the steel pits is evidently limited, however, since some chemical attack continues to occur.

Despite the fact that cracking occurs in both LC and HC chromium during firing, the LC chromium seems to offer advantages over HC chromium. For LC chromium, the density of major cracks is lower than with HC. Furthermore, the numerous fine microcracks that occur between the major chromium cracks in HC are absent in LC. These microcracks, which evolve from the initial embedded cracks during firing, serve as a porous network to promote gas-steel reaction zones beneath the chromium to exacerbate chromium spallation.

Mechanical wear plays a role in the spallation of LC and HC chromium on the 155-mm specimens in contrast to the HC chromium plated 120-mm where thermochemical effects appear to dominate. The conclusion that the spallation of LC chromium on the 155-mm specimens is substantially mechanical in nature is based on evidence of surface wear and the nature of the crack patterns in the chromium. The spallation in the XM297 is seen to be a gradual process with spallation growing from the vicinity of the large cracks that form perpendicular to the wear direction, rather than by spallation of entire islands of chromium that occur with the LC chromium 155-mm case. This may be due to the high density of embedded cracks in the HC chromium. Severe wear occurs on the top surface of the LC chromium on the M199 and

accompanies the spallation on the lands; there is far less spallation in the grooves. Similarly, there is more spallation on the lands of the M297 than in the grooves, but the difference is less dramatic.

The mechanical wear in the 155-mm is probably due to the sliding of the metal rotating bands. Nylon is used for the 120-mm rounds and may account for the lack of any apparent wear in these specimens. The sliding mode of chromium spallation has been studied (ref 9) and is consistent with the present observations on the tendency to spall by failure near the interface and the alignment of major chromium cracks perpendicular to the sliding direction. (The lower flame temperatures for standard 155-mm rounds and specimen location along the tube may also be factors in determining the relative importance of chemical and mechanical effects.)

One of the lessons from this study has been well known for over five decades (ref 1): bore protective coatings should be designed to develop a minimum density of coating cracks. The numerous chemically aggressive components in the hot propellant gas show the need for crack minimization and a generally chemically inert coating. In this regard, LC chromium appears to be a reasonable first step for replacing HC chromium. Also, the current effort in sputtering refractory bore coatings should include thermal shock resistance as an essential coating property. For the 155-mm systems, resistance to cracking from sliding wear may be an essential feature for effective coatings.

Among the new lessons offered by the present work is that the gray reaction products that occur at the fine chromium crack tips provide a means of sampling the chemical erosion process occurring elsewhere on unprotected steel within the tube. An evaluation of these products may also serve as a viable tool for assessing effects of varying propellant compositions. In the present work, analysis of these gray reaction products has given new information on the origin of the damage that undermines the chromium plate.

As stated in the introduction, gun bore erosion remains an empirical science and other factors besides those discussed here may be contributing to coating loss and spallation. Such factors may become evident as more demanding propellants are introduced. For example, melting of the coating is a possible mechanism for coating loss at high turbulence regions such as pits, or with higher propellant flame temperatures. Another mechanism for coating loss is interface degradation from high-temperature interdiffusion of the coating material and steel constituents (ref 14). A further concern is that coatings may become embrittled by absorption of propellant gas products, such as hydrogen and oxygen, which would adversely affect resistance to thermal shock and sliding wear.

REFERENCES

1. Burlew, J.S., ed., "Hypervelocity Guns and the Control of Gun Erosion," Summary Technical Report of the National Defense Research Committee, Division 1, Office of Scientific Research and Development, Washington, DC, 1946.

2. Ahmad, I., "The Problem of Gun Barrel Erosion-An Overview," *Gun Propulsion Technology*, (L. Stiefel, ed.), Progress in Astronautics and Aeronautics Series, AIAA, Washington, DC, 1988, pp. 311-355.

3. *Proceedings of the Sagamore Workshop on Gun Barrel Wear and Erosion*, Wilmington, DE, 29-31 July 1996, (R.J. Dowding, J.S. Montgomery, U.S. Army Research Laboratory, eds.).

4. Alkidas, A.C., Morris, S.O., and Summerfield, M., *Journal of Spacecraft and Rockets*, Vol. 13, No. 8, August1976, pp. 461-465.

5. Underwood, J.H., Parker, A.P., Cote, P.J., and Sopok, S., *Transactions of the ASME*, Vol. 121, February 1999, pp. 116-120.

6. Brittain, C.P., and Smith, G.C., *Transactions of the Institute of Metal Finishing*, Vol. 33, 1956, pp. 289-300.

7. Kamdar, M.H., Campbell, A., and Brassard, T., Technical Report ARLCB-TR-78012, Benet Laboratories, Watervliet, NY, August 1978, p. 11.

8. Billington, R., private communication, PM-TMAS, Picatinny Arsenal, NJ.

9. Gawne, D.J., *Thin Solid Films*, Vol. 118, 1984, pp. 385-393.

10. Botstein, O., and Arone, R., *Wear*, Vol. 142, 1991, pp. 87-95.

11. Sopok, S., "Benet Laboratories M242/M919 Multidisciplinary Analyses," ARDEC Special Publication for CCAC Commander, 16 April 1992.

12. Sims, C., Stoloff, N., and Hagel, W., eds., *Superalloys II*, John Wiley and Sons, NY., 1987.

13. Cote, P.J., Kendall, G., and Todaro, M., to be published.

14. Cote, P.J., to be published.

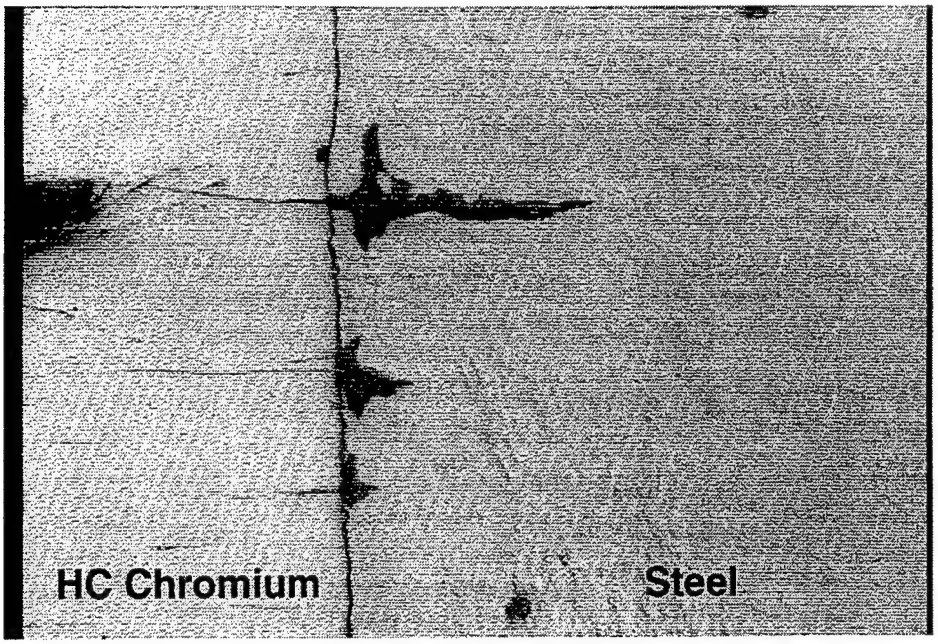

Figure 1. Micrograph of an unetched section of specimen 1 showing the chemical attack on steel. Note fissures are present within the steel reaction products.

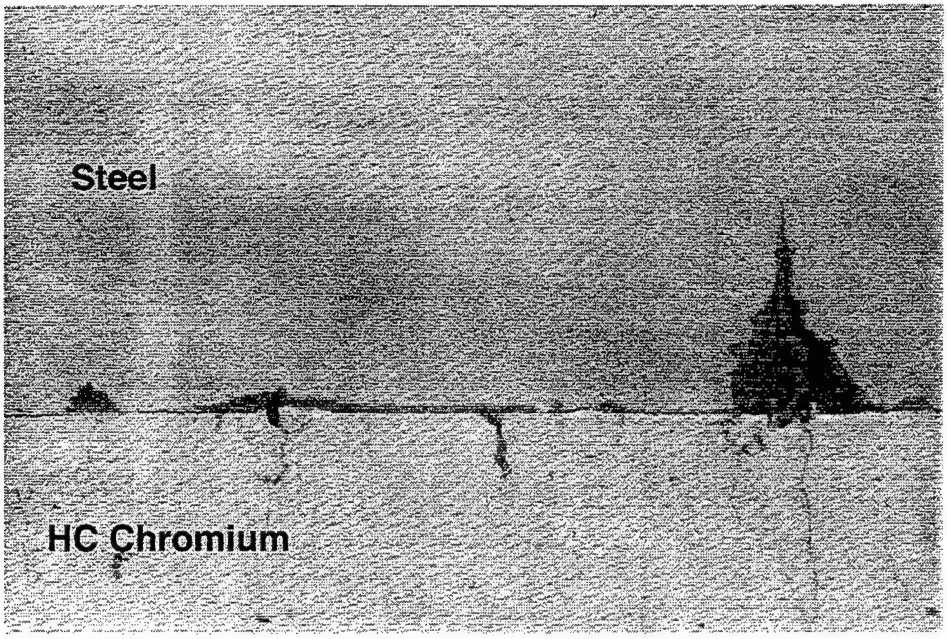

Figure 2. Micrograph of an unetched section of specimen 2 showing the chemical attack along the interface.

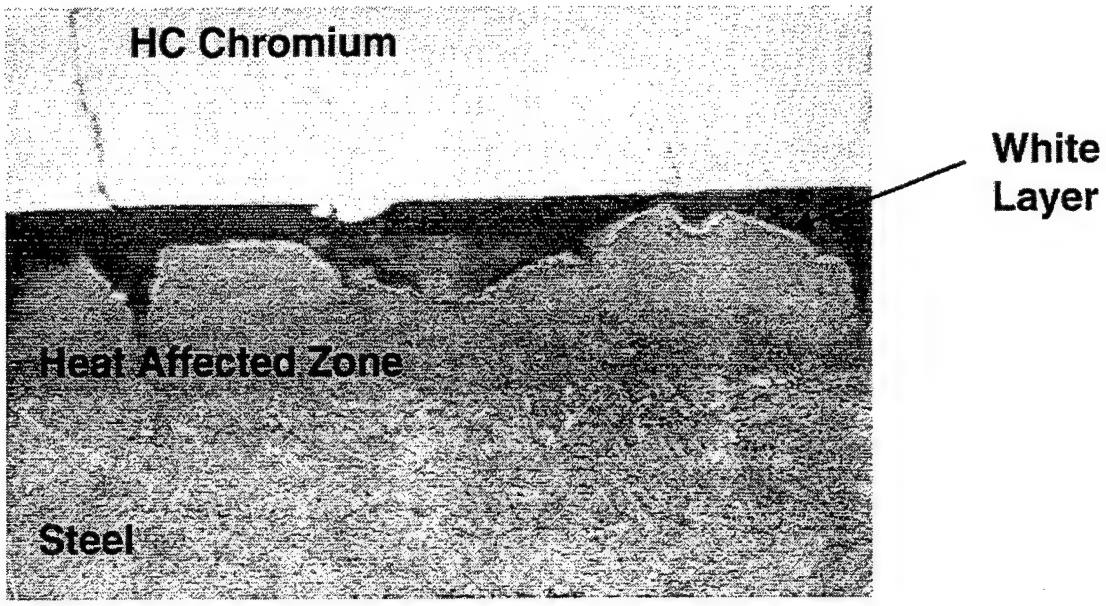

Figure 3. Micrograph of an etched section of specimen 2 showing dissolution of reaction products, heat-affected zone, and white layer.

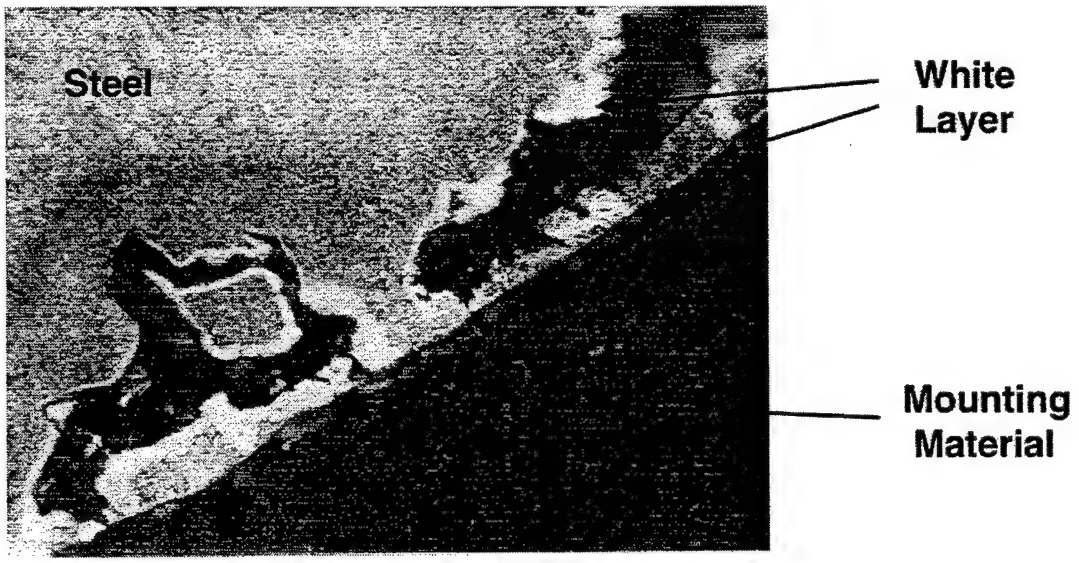

Figure 4. Micrograph of an etched section of specimen 2 where the chromium and an approximately 5-mm layer of steel beneath the chromium had been removed by erosion.

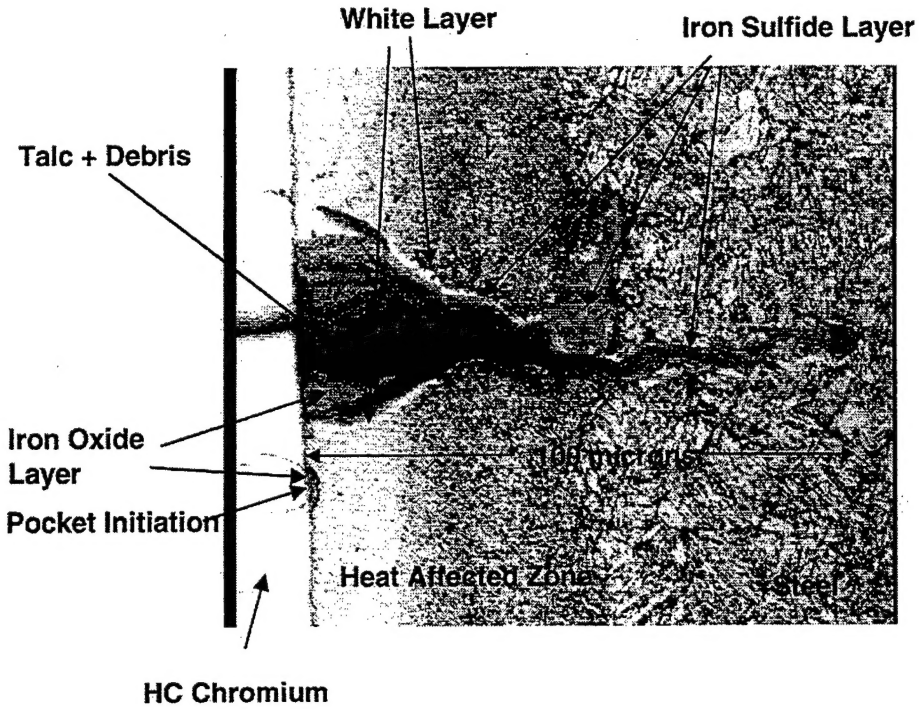

Figure 5. Micrograph of an etched section of specimen 2 indicating the chemical compositions deduced from EDS analysis.

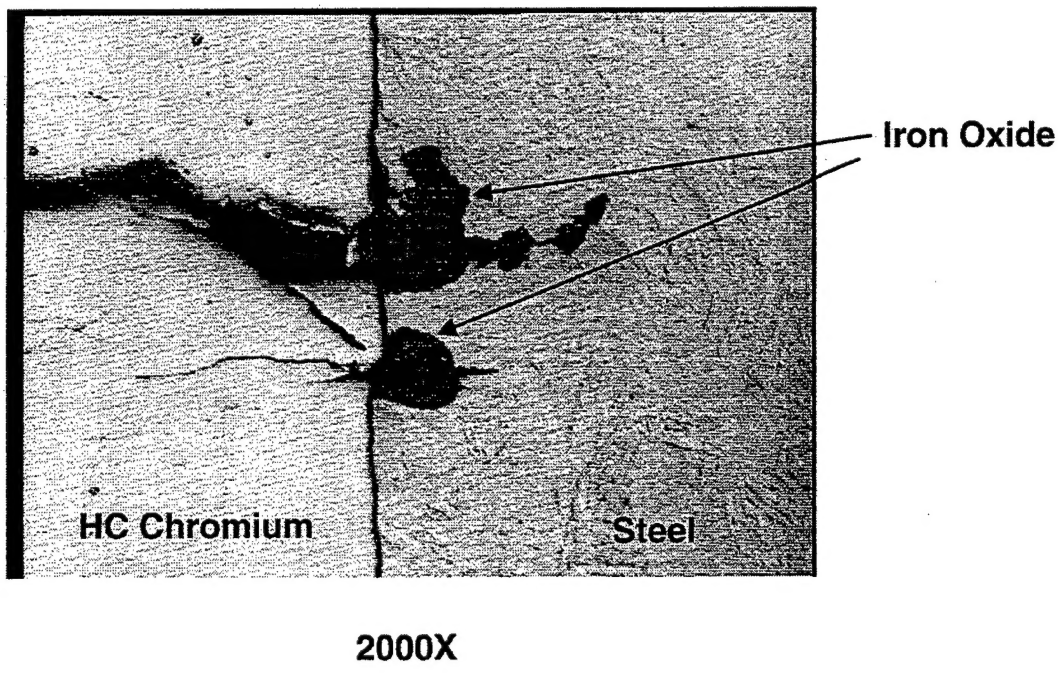

Figure 6. Micrograph of an unetched section of specimen 3 depicting different stages of chemical attack.

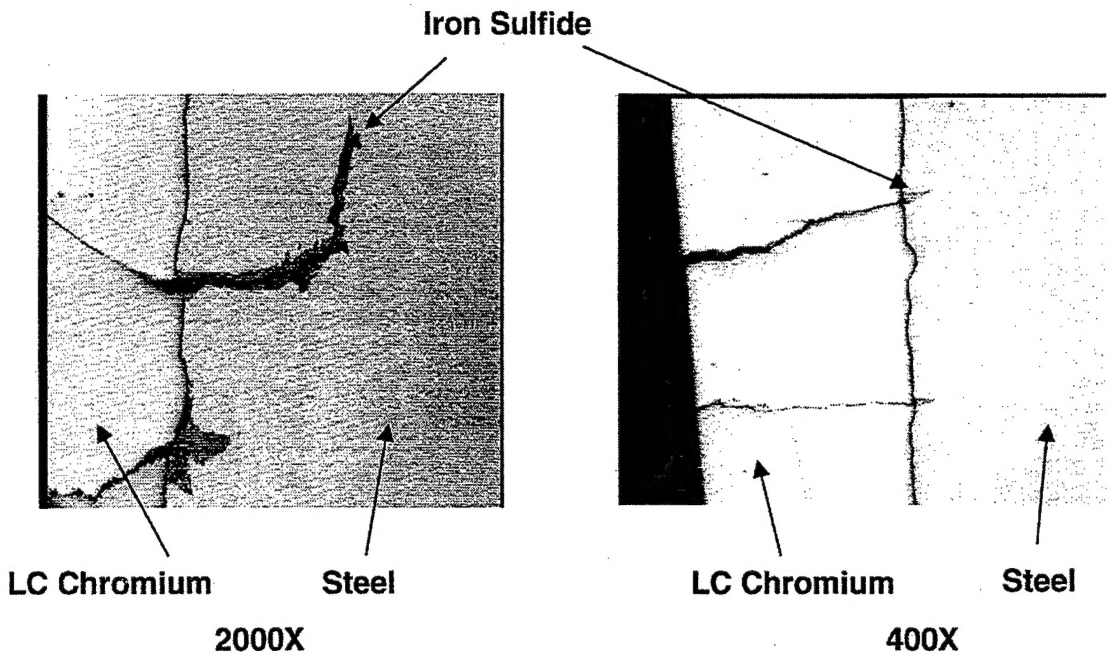

Figure 7. Micrographs of specimen 4 at 2000X and 400X showing initiation and propagation of chemical attack.

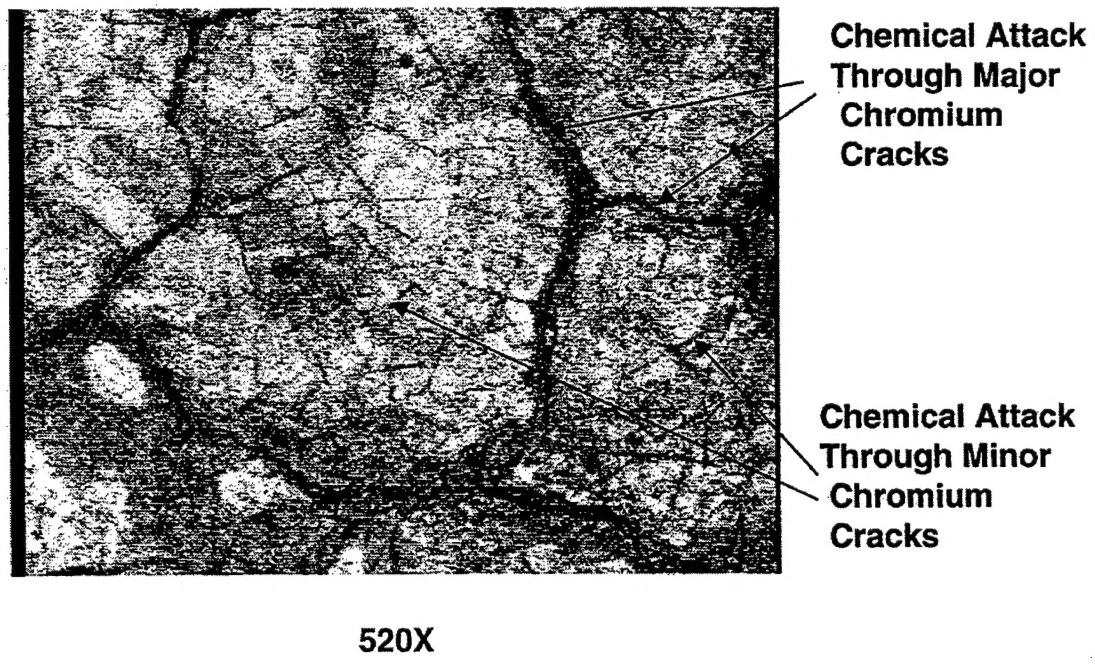

Figure 8. Micrograph of specimen 2 steel/chromium interface plane after electrochemical removal of all chromium in this area. Note the depth of penetration of the corrosion zones into the steel should vary roughly with the widths of the corrosion gaps at the surface.

TECHNICAL REPORT INTERNAL DISTRIBUTION LIST

	NO. OF COPIES
TECHNICAL LIBRARY ATTN: AMSTA-AR-CCB-O	5
TECHNICAL PUBLICATIONS & EDITING SECTION ATTN: AMSTA-AR-CCB-O	3
OPERATIONS DIRECTORATE ATTN: SIOWV-ODP-P	1
DIRECTOR, PROCUREMENT & CONTRACTING DIRECTORATE ATTN: SIOWV-PP	1
DIRECTOR, PRODUCT ASSURANCE & TEST DIRECTORATE ATTN: SIOWV-QA	1

NOTE: PLEASE NOTIFY DIRECTOR, BENÉT LABORATORIES, ATTN: AMSTA-AR-CCB-O OF ADDRESS CHANGES.

TECHNICAL REPORT EXTERNAL DISTRIBUTION LIST

	NO. OF COPIES
DEFENSE TECHNICAL INFO CENTER ATTN: DTIC-OCA (ACQUISITIONS) 8725 JOHN J. KINGMAN ROAD STE 0944 FT. BELVOIR, VA 22060-6218	2
COMMANDER U.S. ARMY ARDEC ATTN: AMSTA-AR-WEE, BLDG. 3022 AMSTA-AR-AET-O, BLDG. 183 AMSTA-AR-FSA, BLDG. 61 AMSTA-AR-FSX AMSTA-AR-FSA-M, BLDG. 61 SO AMSTA-AR-WEL-TL, BLDG. 59 PICATINNY ARSENAL, NJ 07806-5000	 1 1 1 1 1 2
DIRECTOR U.S. ARMY RESEARCH LABORATORY ATTN: AMSRL-DD-T, BLDG. 305 ABERDEEN PROVING GROUND, MD 21005-5066	 1
DIRECTOR U.S. ARMY RESEARCH LABORATORY ATTN: AMSRL-WM-MB (DR. B. BURNS) ABERDEEN PROVING GROUND, MD 21005-5066	 1
COMMANDER U.S. ARMY RESEARCH OFFICE ATTN: TECHNICAL LIBRARIAN P.O. BOX 12211 4300 S. MIAMI BOULEVARD RESEARCH TRIANGLE PARK, NC 27709-2211	 1
COMMANDER ROCK ISLAND ARSENAL ATTN: SIORI-SEM-L ROCK ISLAND, IL 61299-5001	 1
COMMANDER U.S. ARMY TANK-AUTMV R&D COMMAND ATTN: AMSTA-DDL (TECH LIBRARY) WARREN, MI 48397-5000	 1
COMMANDER U.S. MILITARY ACADEMY ATTN: DEPT OF CIVIL & MECH ENGR WEST POINT, NY 10966-1792	 1
U.S. ARMY AVIATION AND MISSILE COM REDSTONE SCIENTIFIC INFO CENTER ATTN: AMSAM-RD-OB-R (DOCUMENTS) REDSTONE ARSENAL, AL 35898-5000	 2
COMMANDER U.S. ARMY FOREIGN SCI & TECH CENTER ATTN: DRXST-SD 220 7TH STREET, N.E. CHARLOTTESVILLE, VA 22901	 1

NOTE: PLEASE NOTIFY COMMANDER, ARMAMENT RESEARCH, DEVELOPMENT, AND ENGINEERING CENTER, BENÉT LABORATORIES, CCAC, U.S. ARMY TANK-AUTOMOTIVE AND ARMAMENTS COMMAND, AMSTA-AR-CCB-O, WATERVLIET, NY 12189-4050 OF ADDRESS CHANGES.